

Spatial evolution of an ion beam created by a geometrically expanding low-pressure argon plasma

C. S. Corr,^{1,a)} R. W. Boswell,¹ C. Charles,¹ and J. Zanger²

¹Space Plasma, Power and Propulsion Group, The Australian National University, Canberra 0200, Australia

²German Aerospace Center, Institute of Combustion Technology, Pfaffenwaldring, 70569 Stuttgart, Germany

(Received 17 April 2008; accepted 13 May 2008; published online 6 June 2008)

The spatial distribution of an ion beam—created at the interface of a small diameter plasma source and much larger diameter diffusion chamber—is studied in a low-pressure inductively coupled plasma using a retarding field energy analyzer. It is found that the ion beam density decays axially and radially in the diffusion chamber following the expansion of the plasma from the source region. The radial distribution of the ion beam indicates that the acceleration region has a convex shape and is located just outside the source exit, giving rise to a hemispherical plasma expansion into the diffusion chamber. © 2008 American Institute of Physics. [DOI: 10.1063/1.2938720]

The past few years have seen increased activity in the study of plasma expansion from various low-pressure plasma sources (helicon, inductively and capacitively coupled, capillary, and electron cyclotron).^{1–14} The process of plasma expansion depends on many parameters, such as the geometry, magnetic field configuration, plasma production mechanism, gas pressure, and input power. As a result of the plasma expansion, an accelerated ion population is often observed downstream of the ionization region. In some experiments, the acceleration is caused by the formation of a current free double layer created when a strongly diverging magnetic field is applied.^{1,7} In other experiments, the acceleration is due to the expanding physical geometry, which induces strong electric field gradients.^{8,9} This serves to retard electrons inside the plasma source and to accelerate ions from the source into the diffusion chamber. We⁹ recently showed that in a geometrically expanding plasma, changing the ratio of the cross-sectional areas of the source tube and diffusion chamber can control the ion acceleration. It was shown that a smaller source tube radius leads to a higher potential gradient and hence to a higher accelerated ion beam energy. In that work a double layer was not observed.

Of particular interest to the propulsion community is the spatial distribution of the accelerated ion beam downstream of the plasma source. Charles¹⁵ showed that the ion beam generated by a double layer in their argon helicon double layer thruster experiments is only weakly divergent. This is partly due to the creation of the double layer in the source, which establishes an ion beam with an initial diameter equal to that of the source. Second, it has previously been shown that the ion beam is detached from the magnetic field at approximately $z=7$ cm from the source exit and the ion beam maintains the diameter of source tube.¹⁶

In the present letter, we investigate the radial variation of an ion beam observed in a low-pressure geometrically expanding plasma. Our aim is to study the basic principles of ion beam generation in a simple geometrically expanding plasma system.

A schematic of the low-pressure plasma reactor (Bilby) is shown in Fig. 1. For this work, the plasma reactor consists

of the 4.5 cm diameter, 20 cm long source tube with one end connected to a 14 cm diameter, 28 cm long aluminium diffusion chamber. At the other end of the source tube, a floating metal vacuum connection is attached and argon gas enters the system. The air-cooled three-loop antenna is powered through a close-coupled pi-type matching network by an rf power supply operating at 13.56 MHz and capable of delivering up to 500 W forward power. A pumping system consisting of a turbomolecular and a rotary pump is connected to the sidewall of the diffusion chamber and routinely achieves base pressures of 10^{-6} mTorr. The gas pressures are determined by controlling the flow of argon via a needle valve. Typical operating pressures were from 0.2 to 5 mTorr and were measured with an ionization gauge and convectron mounted on the diffusion chamber.

In this work, a grounded retarding field energy analyzer (RFEA) mounted on the side of the diffusion chamber 6.6 cm from the source/diffusion chamber interface and an RFEA moveable along the z axis with the aperture hole facing the source were used to determine the ion energy distribution function (IEDF). The data acquisition technique applied for this work is similar to that in Ref. 17 for a Langmuir probe. The bias applied to the discriminator was supplied by an isolated bipolar voltage source swept at 12.5 Hz from 100 to 0 V. The repeller was biased at -90 V,

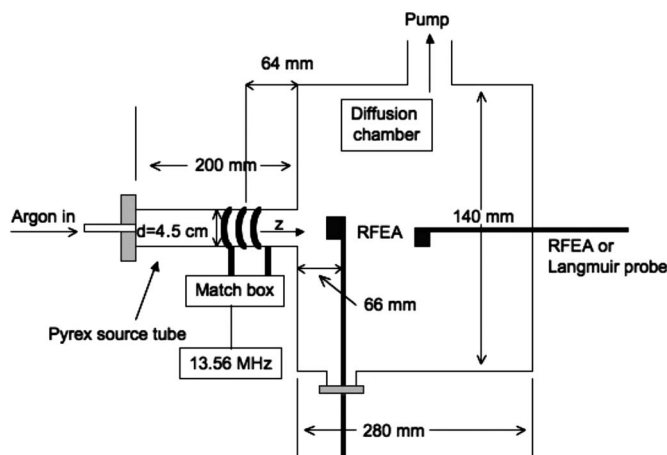


FIG. 1. A schematic of the plasma device.

^{a)}Electronic mail: cormac.corr@anu.edu.au.

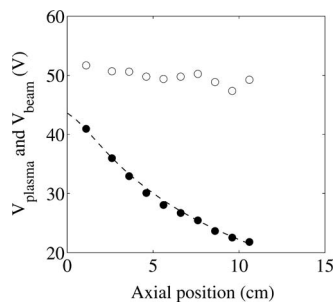


FIG. 2. The axial evolution of the plasma (solid circles) and beam (open circles) potentials at 0.6 mTorr and 100 W. The line corresponds to a calculated $R_0^2/R_0^2+z^2$ plasma expansion.

the secondary electron suppressor at -12 V and the collector at -3.2 V. The current signal from the collector was passed through a 10 k Ω resistor and an isolation amplifier, which were integrated into a strictly grounded analyzer supply box. The voltage signal was then fed into two resonant circuits, which acted as a filter for low-frequency plasma instabilities and as a differentiator. The data acquisition was managed by a National Instruments SCB-68 shielded connector board, which transferred the incoming signals to a National Instruments PCI 6221 DAQ board. This provided a data acquisition at 16 bits with a sampling rate up to 250 kS s^{-1} . To reduce random noise, the measurements were averaged over 100–700 single shots depending on the signal quality. From the IEDF, the local plasma potential, the beam energy, and the beam and plasma density were determined. The probe analysis here follows the methods described by Charles *et al.*¹⁸ and Plihon *et al.*⁶ For this work, the beam potential is taken to be the potential relative to zero discriminator bias at which the beam feature appears in the IEDF.

The axial variation of the plasma potential (solid circles) and beam potential (open circles) for the 4.5 cm diameter source tube of length 20 cm are presented in Fig. 2. The axial position $z=0$ cm corresponds to the source/diffusion chamber interface. It was not possible to go beyond this position, as the RFEA head was larger than the source tube diameter. Figure 2 shows that the ion beam is formed near the interface and its energy (≈ 50 eV) remains constant along the axis of the diffusion chamber. The plasma potential decreases into the diffusion chamber, as was observed for the 6 cm source tube in Corr *et al.*⁹ As in Ref. 9, we consider the plasma to originate from a point source and to expand as $n(z)=n(0) \times (R_0^2/R_0^2+z^2)$, where $n(0)$ is the density at the source/diffusion chamber interface, R_0 is the source tube radius, and z is the axial distance from the interface.¹⁹ The dashed line in Fig. 2 corresponds to a Boltzmann expansion. The ion beam density decreases axially in the diffusion chamber as a result of damping by ion-neutral charge exchange collisions. The charge exchange mean free path for thermal ions in low-pressure plasmas is $\lambda_i(\text{cm})=3/p$, where p is the pressure in millitorr. The velocity dependence of the charge exchange cross section leads a correction factor when estimating the mean free path of a 15 eV ion beam. The effective mean free path is estimated to be $\lambda=\lambda_i/0.7$ (at 1 mTorr, $\lambda=4.3$ cm). The ion beam could be detected over approximately two mean free paths which is similar to previous work.^{6,14}

The raw IEDF data obtained at $r=0, 2.5,$ and 5 cm are shown in Fig. 3 for a gas pressure of 1 mTorr and input power of 100 W. Under these operating conditions, the

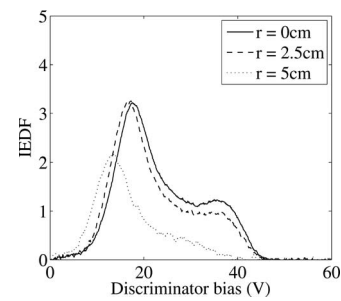


FIG. 3. The IEDFs for $r=0, 2.5,$ and 5 cm at 1 mTorr and 100 W.

plasma density is approximately 10^{12} cm^{-3} in the source and 10^{11} cm^{-3} at $z=6.6$ cm from the interface. All three curves display two peaks; the lower energy peak corresponds to the local plasma potential and the higher energy peak to a higher energy ion population. It appears that the ions generated in the inductively coupled source are accelerated near the source/diffusion chamber interface to supersonic velocities. Although at $r=5$ cm the IEDF has a reduced peak height and lower potentials, the ion beam is still detected indicating that the ion beam is spread across the width of the diffusion chamber. The shift in the ion beam potential near the wall of the diffusion chamber is related to the radial distribution of the plasma potential in the acceleration region.

With the RFEA maintained 6.6 cm from the interface, the RFEA probe was swept from $r=0$ cm to the diffusion chamber edge ($r=7$ cm) to characterise the ion beam and plasma parameters radially. The radial variation of the plasma and beam densities is shown in Fig. 4. The open circles correspond to the ion beam density and the solid circles to the plasma density. For both densities, the radial profile is nearly flat for $r<2$ cm, which corresponds to the radius of the source, and then decreases for $r>2$ cm toward the diffusion chamber wall. Both show a reasonable agreement with a $R_0^2/R_0^2+z^2$ expansion (as indicated by the lines in Fig. 4). The discrepancy may be a result of beam damping. The plasma density is higher than the beam density by about a factor of 6. These profiles show that the accelerated ion beam follows the plasma expansion.

Figure 5(a) shows the radial variation of the plasma and beam potentials. Here the lines correspond to the potentials obtained from the Boltzmann expansion, $V_p(r)=V_p(0)$

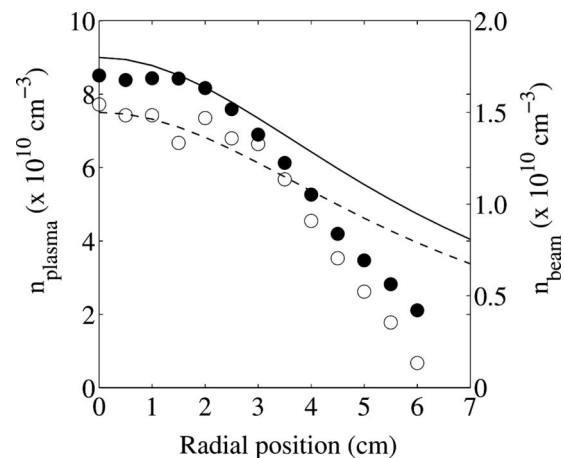


FIG. 4. The radial variation of the plasma (solid circles) and beam (open circles) densities at 1 mTorr and 100 W. The lines correspond to a calculated $R_0^2/R_0^2+z^2$ plasma expansion.

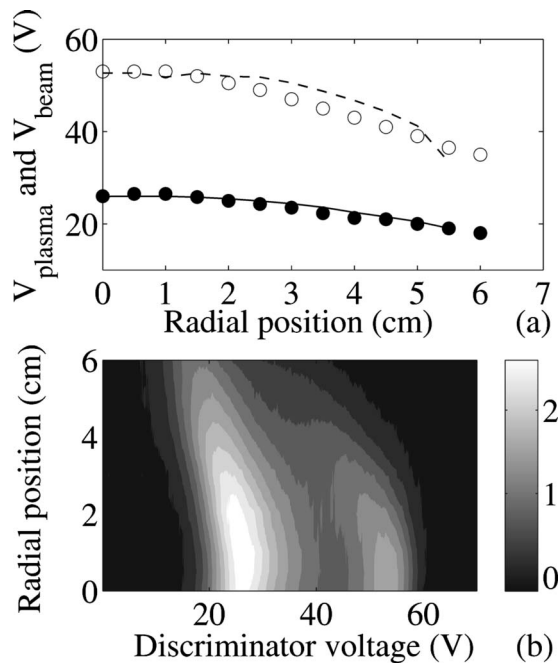


FIG. 5. (a) The radial variation of the plasma (solid circles) and beam (open circles) potentials at 1 mTorr and 100 W. The lines correspond to a Boltzmann expansion calculated from the measured densities in Fig. 4. (b) Contour plot of the IEDFs vs radial position at 100 W and 1 mTorr.

$+T_e \ln [n(r)/n(0)]$. Again, reasonable agreement is observed. This is very different to the results of Charles *et al.*¹⁵ where the ion beam is located in the region of the expansion chamber that mirrors the source tube, i.e., the beam has a low divergence. This indicates that for the present configuration the ion beam is either highly divergent or it expands spherically. Previously, Langmuir probe and RFEA measurements in a multipole confined argon plasma²⁰ displayed a similar plasma expansion.

A contour plot of the radial variation of the IEDF is shown in Fig. 5(b) for a 100 W plasma at 1 mTorr. The plasma potential at $r=0$ cm is ≈ 25 V and decreases to ≈ 16 V at the wall of the diffusion chamber. The beam potential is ≈ 55 V at $r=0$ cm and decays to ≈ 35 V at $r=6$ cm. This spatial change in the potentials shows that the ion beam does follow the plasma as it expands outwards from the source. The supersonic expansion may be caused by a shock at the source exit. It appears that a hemispherical double layer, similar to that observed in electronegative plasma,^{4–6} may be formed in the vicinity of the source exit, which leads to the ion acceleration and the subsequent radial profiles. This is currently under investigation.

The spatial distribution of an ion beam observed in the expansion region of geometrically expanding low-pressure

plasma has been investigated. The acceleration region is near the source/diffusion chamber interface and the ion beam density decays along the axis and across the radius of the diffusion chamber. The measurements reveal that the axial and radial variation of the ion beam follows the expansion of the background plasma from the source tube into the diffusion chamber. This is due to either a hemispherical double layer or the strong electric field gradients occurring at the interface. Although a large beam divergence is observed, this type of propulsion device would be suitable for space propulsion applications due to an increase in power efficiency resulting from the absence of the magnetic field. Further experiments are underway to determine whether a double layer is created at the source/diffusion chamber interface. Due to the dimensions of the experimental apparatus, a nonintrusive technique, such as laser-induced fluorescence or the injection of dust (which would be electrostatically confined in the high-potential region) to visualize the scale length of the potential gradient²¹ is required so as not to perturb any possible double layer formation.

¹C. Charles and R. W. Boswell, *Appl. Phys. Lett.* **82**, 1356 (2003).

²C. Charles, *Plasma Sources Sci. Technol.* **16**, R1 (2007).

³W. M. Manheimer and R. Fernsler, *IEEE Trans. Plasma Sci.* **29**, 75 (2001).

⁴N. Plihon, C. S. Corr, and P. Chabert, *Appl. Phys. Lett.* **86**, 091501 (2005).

⁵P. Chabert, A. J. Lichtenberg, and M. A. Lieberman, *Phys. Plasmas* **14**, 093502 (2007).

⁶N. Plihon, P. Chabert, and C. S. Corr, *Phys. Plasmas* **14**, 013506 (2007).

⁷K. P. Shamrai, Y. V. Virko, V. F. Virko, and A. I. Yakimeno, Proceedings of the 42nd AIAA, 2006 (unpublished), p. 2006/4845.

⁸A. Dunaevsky, Y. Raitses, and N. J. Fisch, *Appl. Phys. Lett.* **88**, 251502 (2006).

⁹C. S. Corr, J. Zanger, R. W. Boswell, and C. Charles, *Appl. Phys. Lett.* **91**, 241501 (2007).

¹⁰A. Aanesland and C. Charles, *Phys. Scr.*, T **122**, 023306 (2005).

¹¹N. Plihon, C. Corr, P. Chabert, and J. L. Raimbault, *J. Appl. Phys.* **98**, 023306 (2005).

¹²P. Chabert, N. Plihon, C. S. Corr, J. L. Raimbault, and A. J. Lichtenberg, *Phys. Plasmas* **13**, 093504 (2006).

¹³A. Fruchtman, *Phys. Rev. Lett.* **96**, 065002 (2005).

¹⁴M. D. West, C. Charles, and R. W. Boswell, *J. Propul. Power* **24**, 134 (2007).

¹⁵C. Charles, *IEEE Trans. Plasma Sci.* **33**, 336 (2005).

¹⁶F. N. Gesto, B. D. Blackwell, C. Charles, and R. W. Boswell, *J. Propul. Power* **22**, 24 (2006).

¹⁷K. Takahashi, C. Charles, R. W. Boswell, T. Kaneko, and R. Hatakeyama, *Phys. Plasmas* **14**, 114503 (2007).

¹⁸C. Charles, A. W. Degeling, T. Sheridan, J. H. Harris, M. A. Lieberman, and R. W. Boswell, *Phys. Plasmas* **7**, 5232 (2000).

¹⁹K. T. A. L. Burn, W. J. Goedheer, and D. C. Schram, *J. Appl. Phys.* **90**, 2162 (2001).

²⁰C. Charles, *J. Vac. Sci. Technol. A* **11**, 157 (1993).

²¹A. Barkan and R. L. Merlino, *Phys. Plasmas* **2**, 3261 (1995).